



**HAL**  
open science

## Deformation capacity of fresh cement pastes

Y. El Bitouri

► **To cite this version:**

Y. El Bitouri. Deformation capacity of fresh cement pastes. Korea-Australia Rheology Journal, 2024, 36, pp.99-108. 10.1007/s13367-024-00090-5 . hal-04554323

**HAL Id: hal-04554323**

**<https://imt-mines-ales.hal.science/hal-04554323v1>**

Submitted on 4 Sep 2024

**HAL** is a multi-disciplinary open access archive for the deposit and dissemination of scientific research documents, whether they are published or not. The documents may come from teaching and research institutions in France or abroad, or from public or private research centers.

L'archive ouverte pluridisciplinaire **HAL**, est destinée au dépôt et à la diffusion de documents scientifiques de niveau recherche, publiés ou non, émanant des établissements d'enseignement et de recherche français ou étrangers, des laboratoires publics ou privés.

# 1 **Deformation capacity of fresh cement pastes**

2 Y. El Bitouri

3 *LMGC, IMT Mines Ales, Univ. Montpellier, CNRS, Ales, France*

4 Tel.: +33-4-66-78-53-67

5 E-mail: [youssef.elbitouri@mines-ales.fr](mailto:youssef.elbitouri@mines-ales.fr)

## 6 **Abstract**

7 The deformation capacity conditions several processes in cement based-materials, including  
8 workability and structural build-up. However, the origins of this deformation capacity present  
9 some ambiguities. This paper aims to contribute to improving the comprehension of the  
10 deformation capacity of fresh cement pastes. For this, the effect of water to cement ratio (w/c)  
11 and superplasticizer (SP) dosage on the viscoelastic properties of cement paste is examined using  
12 oscillatory rheology and yield stress measurements. It appears that water to cement ratio affects  
13 slightly the critical strain at the end of the linear viscoelastic domain (LVED) and strongly the  
14 storage modulus. The addition of superplasticizer seems to have a strong effect on the critical  
15 strain. In addition, it was shown that the critical strain at the end of the LVED is associated with  
16 strong physical forces (colloidal forces enhanced by early hydrates formation), while the  
17 transition strain at the flow onset is due to large structural reorganizations.

18 **Keywords:** *yield stress, admixture, rheology, storage modulus, critical strain*

## 19 **1 Introduction**

20 The comprehension of the rheological behavior of fresh cement-based materials is essential to  
21 control certain processes such as pumping, multi-layer casting, and formwork pressure. This  
22 rheological behavior displays various complexities including yielding, structural build-up, non-  
23 linearity, and chemical evolution (dissolution of anhydrous cement and formation of hydrates).  
24 Under shear, fresh cement pastes generally display a viscoelastic behavior involving the  
25 deformation capacity.

26 The characterization of the viscoelastic properties of fresh cement paste can be performed by  
27 several procedures such as dynamic mode rheology (small amplitude oscillation strain) [1–6], and  
28 transient mode rheology (yield stress measurement [5,7–9] or creep/recovery technique [10]).  
29 These procedures can be used to understand different phenomena including the setting [11], the  
30 structural-build-up [2,3] and the effect of superplasticizer [1]. Dynamic mode rheology includes  
31 strain sweep, frequency sweep and time sweep procedures and seems suitable to probe the  
32 microstructure of fresh cement paste in order to investigate the deformation capacity. It consists  
33 on the measurement of the viscoelastic properties such as the storage (or elastic) modulus  $G'$ , the  
34 loss (viscous) modulus  $G''$  and other relevant parameters (critical strain, phase angle, oscillation  
35 stress...). Frequency sweep mode is generally carried out to study the cement paste stability [12],  
36 while time sweep mode is more suitable to examine the structural build-up during the dormant  
37 period of the cement hydration [2,3,5]. Strain (or stress) sweep mode can be performed to examine  
38 the microstructure of cement paste and can give information concerning the network of cement  
39 particles and the forces acting inside this network. It allows the linear viscoelastic domain (LVED)  
40 to be determined. In this domain, the storage ( $G'$ ) and loss ( $G''$ ) moduli remain almost constant  
41 as a function of strain. The end of the LVED is associated with a critical strain of the order of  
42 few hundredths ( $10^{-3}$  to  $10^{-2}$  %) [1,6,8,11], while the transition solid/liquid ( $G' = G''$ ) at the flow  
43 onset is associated with a large strain (few %). Nachbaur et al. [11] used this procedure to examine  
44 the evolution of the structure of cement and pure tricalcium silicate ( $C_3S$ ) pastes during the setting  
45 process. According to these authors, the critical strain of the cement paste is very small and of

46 the order of  $3 \cdot 10^{-2}$  %, which suggests that the forces acting between cement particles are attractive  
47 physical forces associated with the formation of early-hydrates (calcium silicate hydrates C-S-H)  
48 at the contact points between particles.

49 Transient mode includes yield stress measurement and creep/recovery procedure and can be also  
50 used to examine the viscoelastic behavior of cement paste. The yield stress measurement is often  
51 carried out using the stress growth procedure which allows the static yield stress to be measured  
52 [7,9,13,14]. It consists on the application of a very low and constant shear rate ranging from 0.001  
53 to  $0.01 \text{ s}^{-1}$  (depending on the rheometer sensitivity) and on the measurement of the shear stress  
54 evolution as a function of time (or strain). For cement paste, the rheological tool suitable for this  
55 experiment is Vane geometry. The typical curve consists of two domains. The first domain is  
56 related to the elastic behavior in which the shear stress increases linearly with time (or strain:  $\tau =$   
57  $G\gamma$ ) until reached a peak followed by the second domain (viscous regime) corresponding to a  
58 plateau in which the shear stress remains almost constant with time (steady state flow). The peak  
59 defines the static yield stress corresponding to the flow onset. According to Roussel et al. [15],  
60 the yield stress originates from colloidal interactions and direct contacts between cement particles  
61 that contributes to form a network of interacting particles able to withstand the applied stress. The  
62 strain associated with the static yield stress is usually of the order of few percentages and is  
63 attributed to the soft colloidal network [8]. In addition, as reported by Roussel et al. [8] and  
64 Fourmentin et al. [16], the shear stress-shear strain curve can display an abrupt change of the  
65 slope in the very first stages of shearing process. In fact, for a very low shear strains, the shear  
66 stress increases very quickly with the shear strain which could characterize a very stiff material  
67 [8,16]. This slope change is associated with a rigid critical strain which could be associated to the  
68 breakage of early hydrates (C-S-H) bridges between cement particles [8,16], while the peak is  
69 attributed to the rupture of a soft colloidal network.

70 Moreover, the deformation capacity is affected by time. In fact, fresh cement paste exhibits a  
71 time-dependent behavior characteristic of flocculated suspensions. However, this behavior cannot  
72 be referred as thixotropic since it is not completely reversible due to chemical reactions. This is  
73 described by a structural build-up that affect the deformation capacity of the connections between

74 cement particles originating from flocculation and bridging effect [2,5,17–20]. In fact, the  
75 structural build-up is originated from flocculation which leads to the formation of a percolated  
76 network and from bridging effect induced by the formation of early hydrates at the surface of  
77 cement particles [3,8,21–23]. Mostafa and Yahia [3] performed time sweep measurements to  
78 quantify the structuration of cement pastes by monitoring the evolution of both storage modulus  
79 and phase angle. They found that the structural changes at rest can be described by a percolation  
80 time corresponding to the time needed to form colloidal percolated network, while the linear  
81 increase at rest of the storage modulus within the dormant period can describe the chemical  
82 rigidification rate of formed network. Otherwise, the structural build-up at rest can be described  
83 by the increase of the static yield stress with resting time [5,17]. Recently, an interesting study  
84 has been performed by Zhang et al. [21] to quantify the contribution of colloidal forces and early  
85 hydrates (C-S-H) formation on the structural build-up using the evolution of the yield stress. They  
86 showed that the interparticle force, which is the combination of colloidal force and interaction  
87 force between C-S-H particles, is the driving force for the structural build-up. The contribution  
88 of colloidal force appears to be greater in the early period (until 60 min), while the C-S-H force  
89 determines the evolution trend from 30 min at rest [21]. This interparticle force strongly  
90 influences the deformation capacity of the fresh cement paste.

91 Furthermore, the effect of several factors (water to cement (w/c) ratio, SP dosage, supplementary  
92 cementitious materials, time...) on the deformation capacity has been investigated [1,4,5,8,11].  
93 Jiao and De Schutter [1] examined the effect of w/c ratio and superplasticizer dosage on the  
94 critical strain (at the end of the LVED), and found that this critical strain is strongly affected by  
95 superplasticizer dosage, while the effect of w/c ratio is less significant. The critical strain increases  
96 only at high w/c ratio. Jiao and De Schutter [1] explain the effect of w/c ratio by the increase of  
97 the dissolution rate leading to the increase of early hydrates formation, which could also be more  
98 fragile when w/c increases. The effect of superplasticizer on the critical strain is explained by the  
99 entanglement of superplasticizer molecules with each other and the possible enhancement of the  
100 C-S-H bridges. According to the authors, this leads to the improvement of the cohesive bonding

101 between cement, inducing an increase of the deformation capacity of the connections. So, the  
102 shear strain required to initiate the relative movement between particles thus increases [1].  
103 Nevertheless, some ambiguities could be pointed out concerning the origins of the deformation  
104 capacity of fresh cement pastes. In fact, it is often assumed that the deformation capacity involves  
105 two mechanisms occurring at different strains. The critical strain at the end of the LVED (of the  
106 order of  $10^{-2}\%$ ) is attributed to the breakage of early hydrates links between cement particles,  
107 while the transition strain at the flow onset is associated with colloidal network [8,10,11,16].  
108 However, the bridging effect due to the formation of early hydrates at the contact points between  
109 particles remains unclear and depends on several factors (time, dispersion state, composition,  
110 etc...) [23–26]. In addition, a chemically inert materials such as calcite suspension, which have  
111 granular properties close to that of cement paste and sometimes used to mimic the fresh behavior  
112 of cement paste [27,28], display a critical strain at the end of the LVED of the same order of  
113 magnitude [29]. This critical strain cannot be associated with the bridging effect and is attributed  
114 to the inter-floc rupture associated with a weak-link structure, while the transition strain (where  
115  $G' = G''$ ) of the order of few % is associated with the fragmentation of flocs [29]. Moreover, the  
116 effect of solid volume fraction and superplasticizer dosage on the yield stress and on the critical  
117 strain [1,13,15] suggests that the origins of the deformation capacity of fresh cement pastes is  
118 closely related to the interparticle distance.

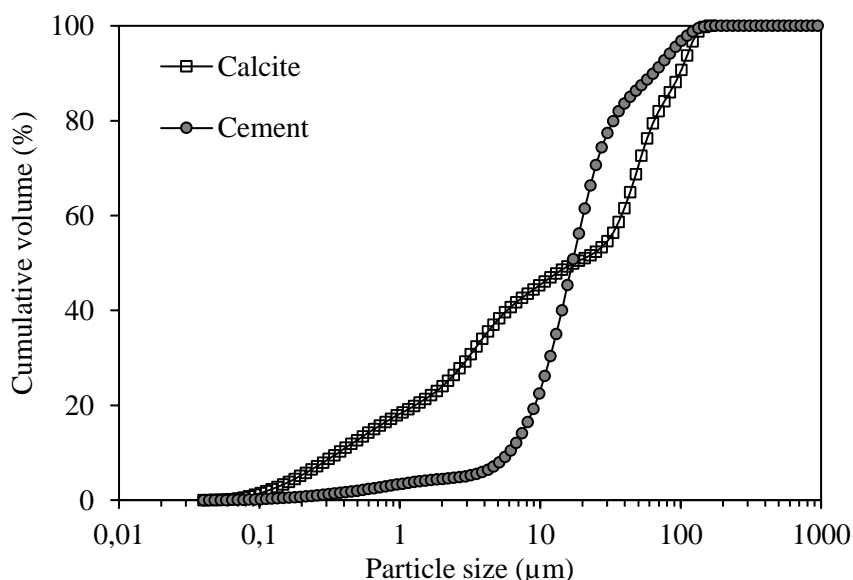
119 The aim of this paper is to investigate the origins of the deformation capacity of fresh cement  
120 pastes. The first part is devoted to the description of the tests which make it possible to  
121 characterize the viscoelastic behavior of fresh cement pastes. Then, the effect of the water to  
122 cement ratio (w/c) and superplasticizer dosage (SP) is examined. Finally, the origins of  
123 deformation capacity of fresh cement pastes are discussed.

124 **2 Materials and methods**

125 **2.1 Materials**

126 An ordinary Portland cement (CEM I-52.5 R) and calcium carbonate (calcite) were used in this  
 127 study. The particle size distributions (Fig. 1) were determined using laser granulometer (LS  
 128 13320-Beckman Coulter). The granular properties are summarized in Table 1.

129 A commercial polycarboxylate-based superplasticizer with dry extract of 19 wt% was used. Three  
 130 dosages of this superplasticizer were used: 0.1, 0.2 and 0.5 wt% of dry substance (by mass of  
 131 cement).



132  
 133

Fig. 1. Particle size distribution of cement and calcite

134

Table 1. Granular properties of cement and calcite

	Cement	Calcite
$d_{10}$ ( $\mu\text{m}$ )	6.6	0.4
$d_{50}$ ( $\mu\text{m}$ )	18.6	19.2
$d_{90}$ ( $\mu\text{m}$ )	70.0	108.4
Density	3.14	2.70
Blaine fineness ( $\text{m}^2/\text{g}$ )	0.44	0.45

135 Cement pastes were prepared with water to cement (w/c) of 0.4, 0.45, 0.5 and 0.6 (Table 2). 200  
 136 g of cement was mixed with deionized water in a planetary agitator (Stuart SS30) for 5 minutes  
 137 at 500 rpm, then the walls of the mixer were scraped to homogenize the mixture (30 seconds),  
 138 and finally the paste was mixed for 1 minute at 1000 rpm. For cement pastes with superplasticizer,  
 139 the cement was first mixed with 90% of water for 5 minutes at 500 rpm, followed by scraping the

140 walls of the mixer (30 seconds), and the required amount of superplasticizer was added to the  
141 remaining water (10%) and the paste was mixed for 1 minute at 1000 rpm.

142 **Table 2. Water to cement ratio and the corresponding solid volume fraction**

water to cement ratio w/c	solid volume fraction $\phi$
0.40	0.44
0.45	0.41
0.50	0.39
0.60	0.35

## 143 **2.2 Rheological measurements**

144 The rheological measurements were performed using a rotational rheometer (AR2000Ex-TA  
145 Instruments) equipped with a four-blade vane geometry (internal diameter = 28 mm, outer cup  
146 diameter = 30 mm, gap = 1 mm).

### 147 **2.2.1 Oscillatory mode**

148 The viscoelastic properties of cement paste can be assessed using oscillatory mode such as stress  
149 sweep procedure. After a pre-shear phase during 30 seconds at a shear rate of  $100 \text{ s}^{-1}$ , an  
150 oscillation stress sweep from 0.01 to 400 Pa is performed with a frequency of 1Hz. It can be noted  
151 that this type of experiment can provide information on the microstructure of the fresh cement  
152 paste [1,4,6]. The typical curve obtained with this oscillation sweep is shown in Fig. 2. The  
153 evolution of storage and loss moduli during this protocol reveals three different regimes: the linear  
154 viscoelastic domain (LVED), the transient yielding zone, and the flow domain. In the linear  
155 viscoelastic domain (LVED), the storage  $G'$  and loss  $G''$  modulus remains almost constant, which  
156 indicates that the microstructure of cement paste is maintained [4]. When  $G'$  is greater than  $G''$ ,  
157 cement paste displays a solid-like behavior, whereas when  $G'$  is lower than  $G''$ , cement paste  
158 exhibits a liquid-like behavior. At the end of the LVED, the moduli begin to drop significantly.  
159 The critical strain at the end of the LVED of order of  $10^{-2}\%$  can be interpreted as a signature of  
160 the breaking of C-S-H links between cement particles [8,10,11]. The intersection of the storage  
161 modulus and the loss modulus curves ( $G' = G''$ ) defines the so-called gel point which characterizes  
162 a solid/liquid transition, i.e. the flow onset. This transition point is associated with a large strain  
163 noted transition strain in Fig. 2.



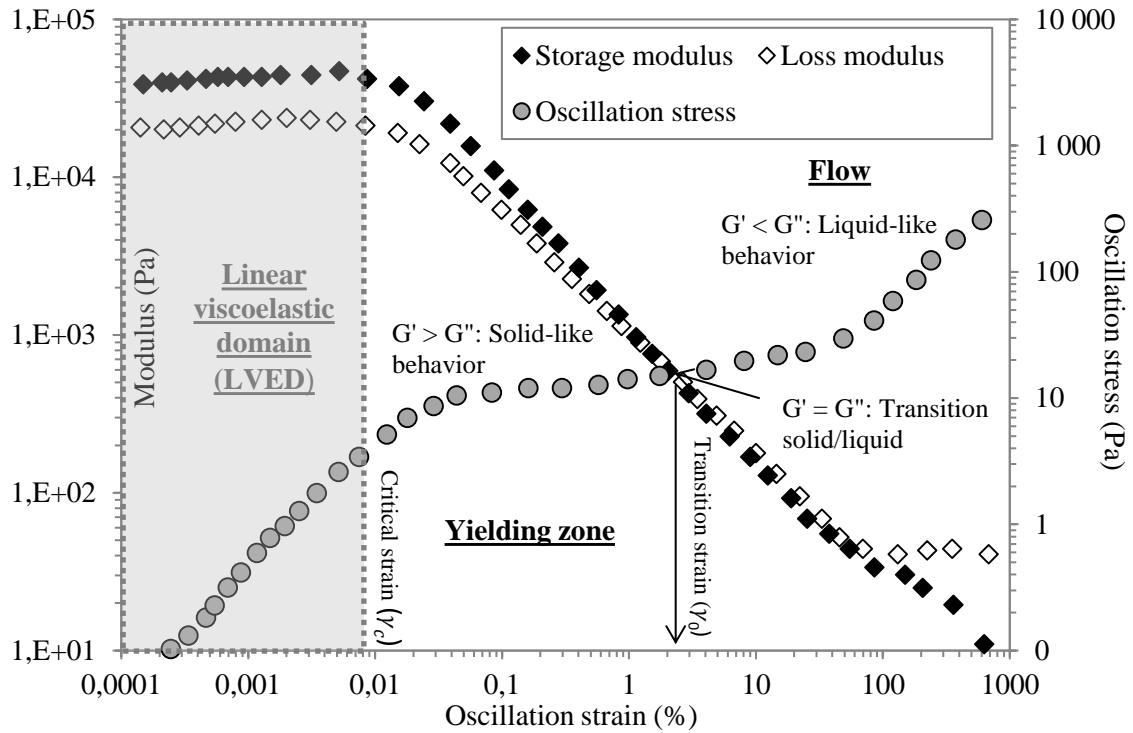
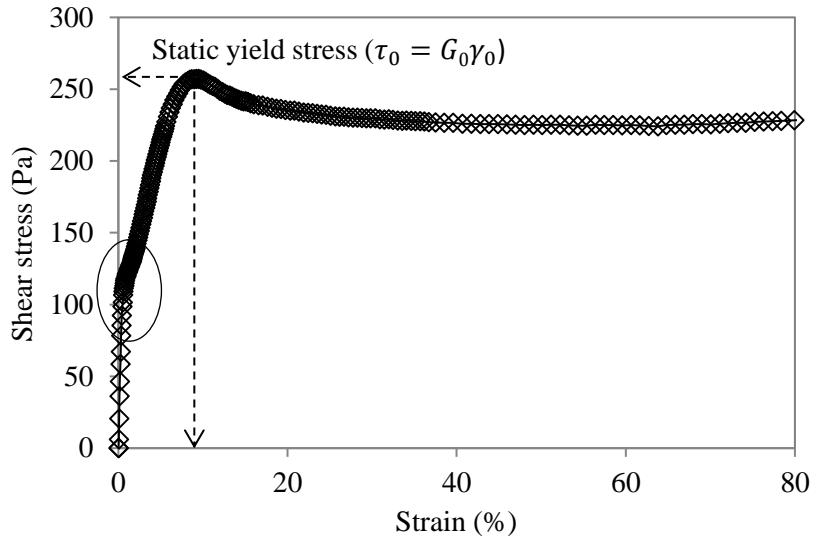


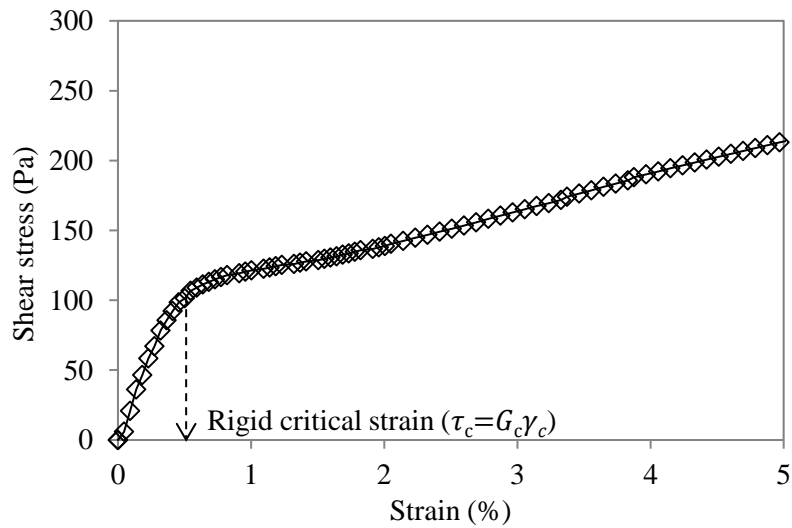
Fig. 2. Typical response to oscillatory stress (or strain) sweep of cement paste (w/c=0.4, 0%SP)

### 2.2.2 Stress growth protocol

The stress growth protocol allows the static yield stress to be measured. It consists of the application of a low and constant shear rate of  $0.005\text{s}^{-1}$  during 180 seconds after a strong pre-shear phase during 30 seconds at  $100\text{ s}^{-1}$  and a resting time. The typical response of cement paste is shown in Fig. 3, where the peak defines the static yield stress and the flow onset (Fig. 3-a). As reported by Roussel et al. [8], the shear stress-shear strain curve can display an abrupt change of the slope in the very first stages of shearing process as shown in Fig. 3-b. This slope change is associated with a rigid critical strain ( $\gamma_c$ ) due to the breakage of C-S-H bridges between particles [8,16]. The peak representing the static yield stress ( $\gamma_0$ ), which characterizes the flow onset, can be the results of the breakage of a soft colloidal network and a rigid network formed by C-S-H bridges between cement particles that was not totally broken when the rigid critical strain was reached or that continuously broken and reformed all along the measurement [8].



(a)



(b)

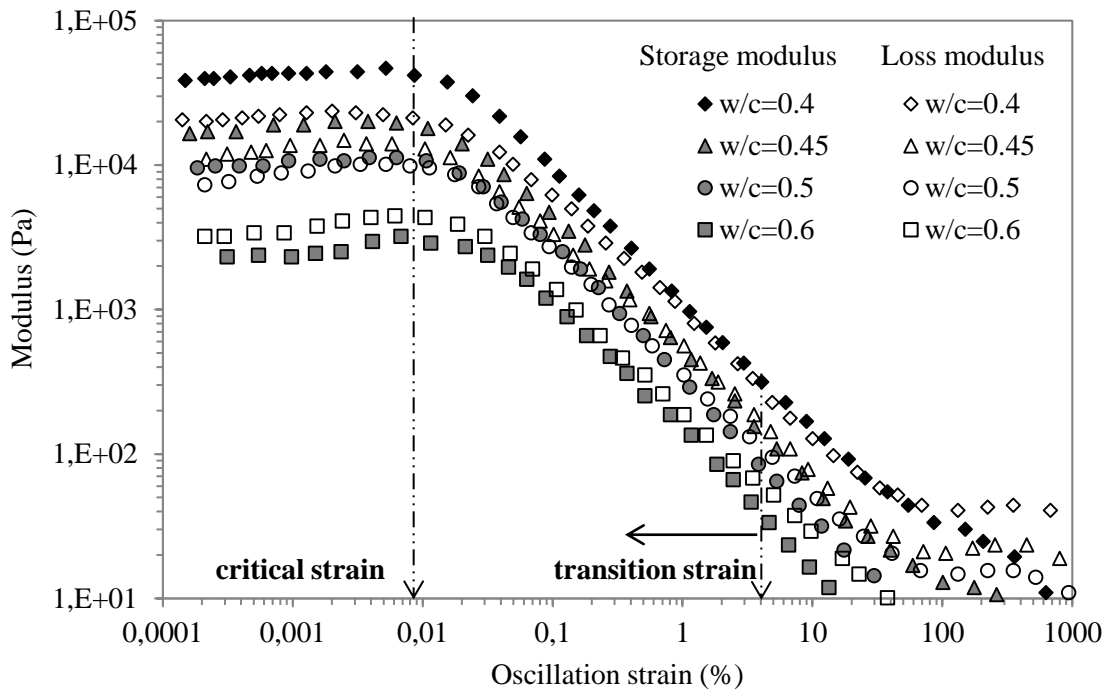
178 Fig. 3. Shear stress as a function of shear strain during a stress growth test on a cement paste with  
 179 a water to cement ratio of 0.4 after 25 min of resting (a) shear strain scale from 0 to 100%, (b) shear  
 180 strain scale from 0 to 5%

### 181 3 Results

#### 182 3.1 Effect of water to cement ratio

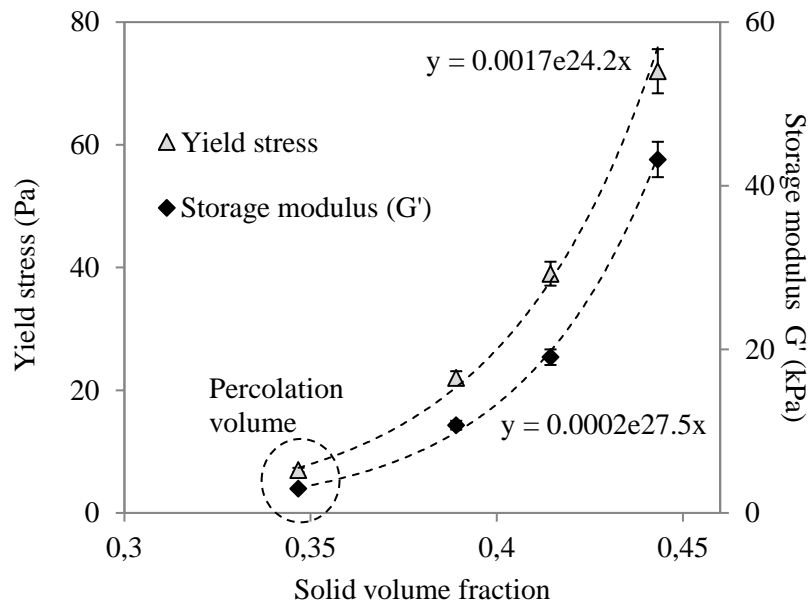
183 Fig. 4 shows the variation of the storage and loss moduli with the oscillation strain for different  
 184 water to cement ratios. In the linear viscoelastic domain (LVED), the storage and loss moduli  
 185 remain almost constant as a function of oscillation strain. The increase of water to cement ratio  
 186 leads to a decrease of both storage and loss modulus. The increase of the storage modulus with

187 water to cement ratio (and solid volume fraction) characterizes the increase of the cement paste  
 188 stiffness and the formation of percolated network [1,30,31] (Fig. 5).



189  
 190 **Fig. 4. Effect of water to cement ratio (w/c) on storage and loss modulus of cement paste**  
 191 In addition, it can be noted that the cement paste displays a solid-like behavior in LVED for low  
 192 w/c ratios, since the storage modulus is greater than the loss modulus. For high water to cement  
 193 ratio, the cement paste can exhibit a liquid-like behavior in LVED.  
 194 This behavior change is related to the dependence of the storage modulus (and the yield stress)  
 195 on solid volume fraction (Fig. 5). The storage modulus (or yield stress)-volume fraction  
 196 relationship reflects the network of interacting particles which percolates under the effect of  
 197 colloidal forces when the percolation volume is reached (Fig. 5) [15]. This particles network  
 198 becomes frictional (direct contacts) with increasing solid volume fraction [15]. This suggests that  
 199 the deformation capacity can be affected by the solid volume fraction which dictates the nature  
 200 of the interaction network (colloidal and/or frictional). As shown in Fig. 4, the critical strain at  
 201 the end of LVED depends slightly on water to cement ratio, but the transition strain seems to  
 202 decrease. The critical strain, often interpreted as a signature of early hydrates (C-S-H) forming  
 203 links between cement particles, corresponds to the shear strain (and the associated shear stress)

204 required to breakdown the contacts and to initiate the relative movement of neighboring cement  
 205 particles [1,8,11,32]. The transition strain ( $\gamma_0$ ) describes the transition solid/liquid. Its decrease  
 206 with decreasing solid volume fraction may reflect the reduction in the strain required to induce  
 207 flow as the number of solid particles decreases. This suggests that this strain would be linked to  
 208 large rearrangements in the suspension.



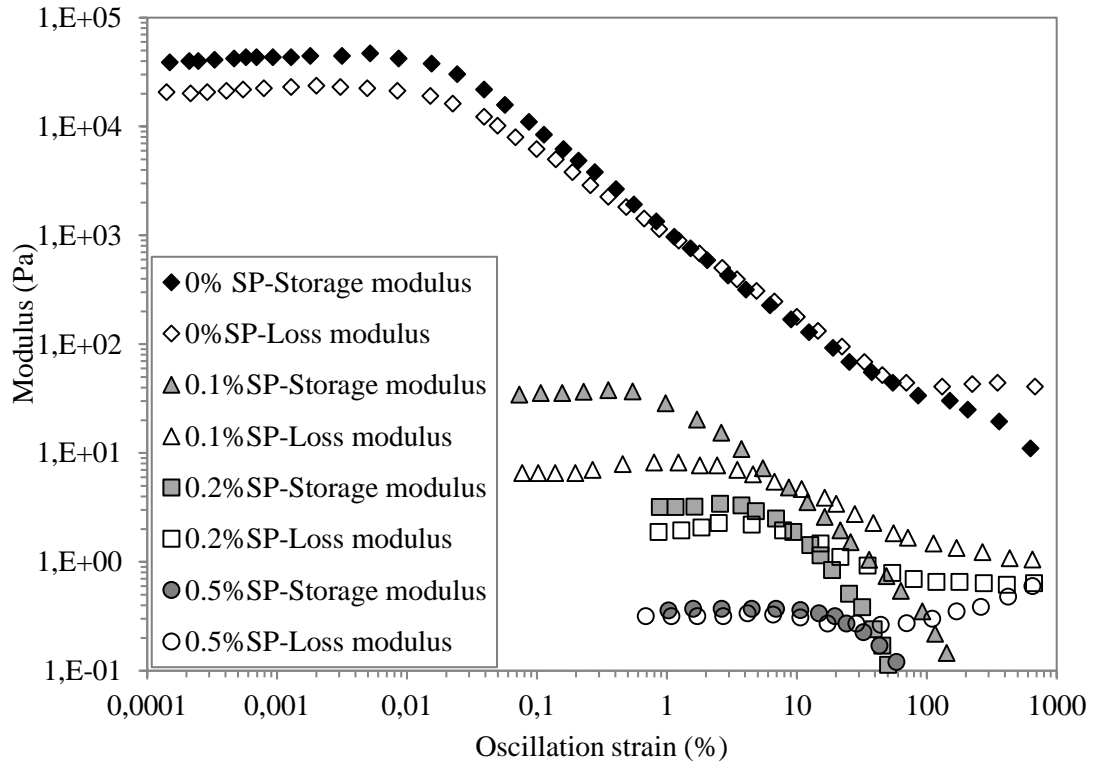
209

210 Fig. 5. Evolution of the yield stress and the storage modulus as a function of solid volume fraction

### 211 3.2 Effect of SP dosage

212 The effect of superplasticizer dosage on the storage and loss moduli of cement paste is presented  
 213 in Fig. 6. It can be noted that the LVED is significantly affected by the addition of superplasticizer.

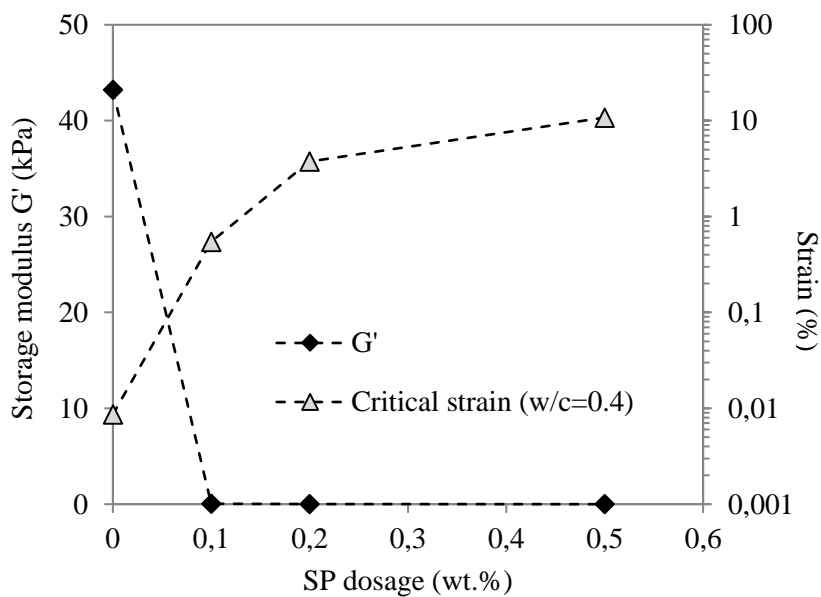
214 The storage modulus decreases strongly with SP dosage. In fact, the addition of superplasticizer  
 215 reduces the magnitude of colloidal interactions [33], and the stiffness of the network of interacting  
 216 particles is thereby decreased.



217  
218

Fig. 6. Effect of superplasticizer dosage on storage and loss modulus of cement paste with w/c of 0.4

219 Moreover, the critical strain ( $\gamma_c$ ), at the end of the LVED, is strongly affected by SP dosage as  
 220 shown in Fig. 6 and Fig. 7. For cement paste without superplasticizer, the critical strain is of the  
 221 order of few  $10^{-2}\%$ , while for cement paste with 0.5% SP, the critical strain is of the order of 10%.  
 222 Others authors reported the same observations [1,3,5], indicating an increase in the deformation  
 223 capacity with the addition of superplasticizer due to the enhanced dispersion of cement particles.

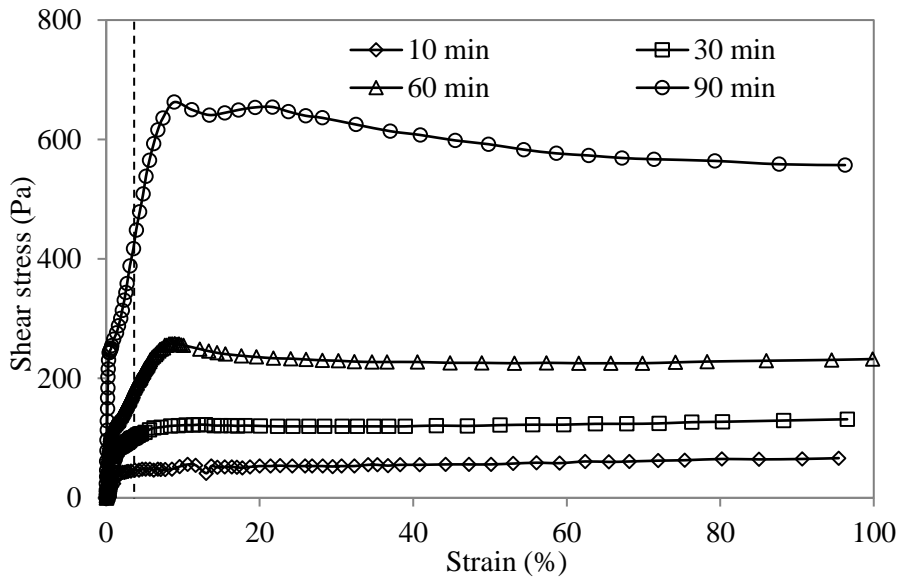


224  
225  
226

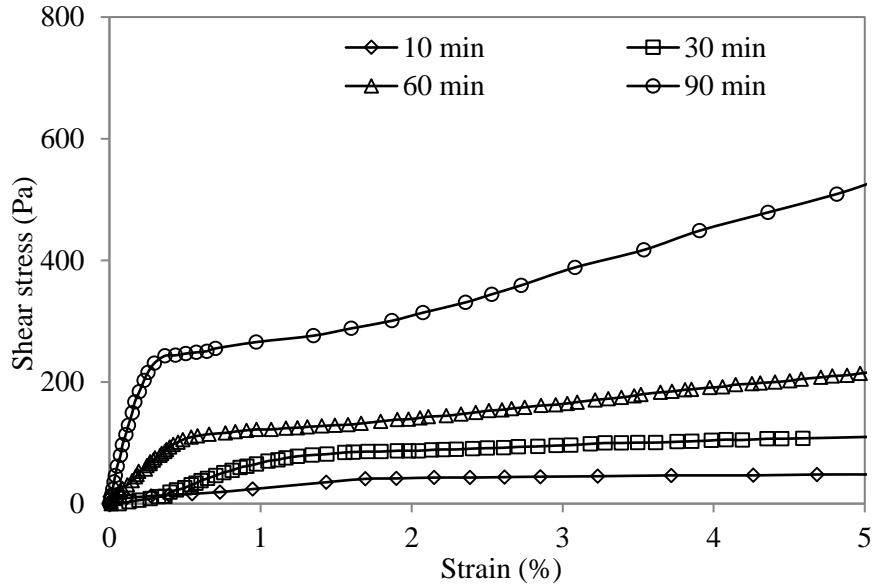
Fig. 7. Evolution of the storage modulus and the critical strain as a function of superplasticizer dosage

227 **3.3 Discussion**

228 As reported by Roussel et al. [8], there is an ambiguity in the literature concerning the origins of  
229 the deformation capacity of fresh cement pastes. The strain ( $\gamma_0$ ) corresponding to the peak of the  
230 shear stress-strain curve obtained by yield stress measurement describes the flow onset (Fig. 8-  
231 a). This strain varies little with the hydration time as shown in Fig. 8-a. Roussel et al. [8] designate  
232 this strain as the largest strain or the soft colloidal strain associated to the colloidal network. In  
233 addition, Roussel et al. [8] and Fourmentin et al. [16] pointed out the existence of a small strain  
234 ( $\gamma_c$ ) in the very first stages of the shearing process during yield stress measurement as shown in  
235 Fig. 8-b, which can be attributed to the rupture of C-S-H bridges between cement particles [8,16].  
236 It can be noted that this small strain slightly decreases with hydration time, and the associated  
237 shear stress increases as shown in Fig. 8-b. This reflects a rigidification of the cement paste  
238 probably due to the formation of hydrates at the contact point between particles.



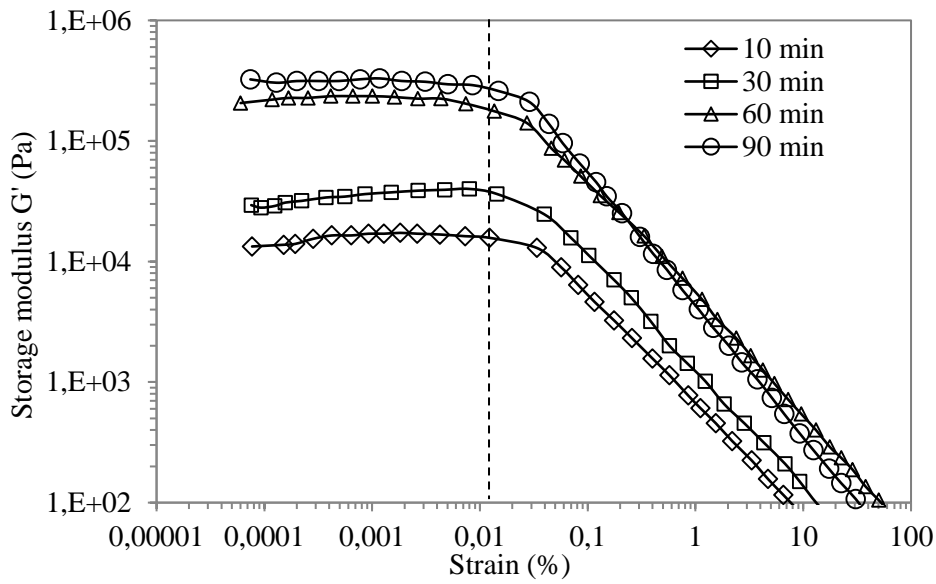
(a)



(b)

239 Fig. 8. Yield stress measurement performed at different times of hydration (cement paste with w/c  
 240 of 0.5: (a) full linear scale, (b) zoom on the first 5% of strain

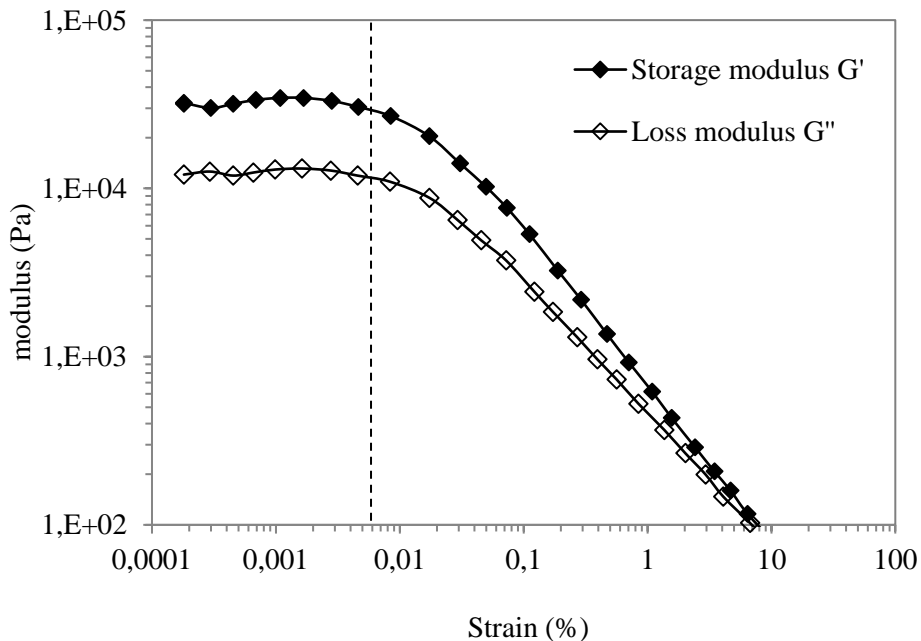
241 The critical strain in oscillatory tests (at the end of the LVED) is also associated to the breakage  
 242 of C-S-H links between cement particles [8]. Nevertheless, the formation of early hydrates at the  
 243 contact points between particles during the dormant period of the cement hydration is not clearly  
 244 elucidated. According to Sujata and Jennings [24], after 10 min of hydration, C<sub>3</sub>S gets covered by  
 245 C-S-H, while Gauffinet et al. [25] rather reported 1 hour of hydration. Nachbaur et al. [11]  
 246 reported that the critical strain remains the same from mixing to after setting suggesting that  
 247 particles are held together by strong physical forces. Fig. 9 shows an example of the evolution of  
 248 the storage modulus as a function of hydration time. It can be observed, as reported by Nachbaur  
 249 et al. [11], that as the hydration progresses, the storage modulus increases but the critical strain  
 250 remains constant. According to Nachbaur et al. [11], just after mixing, there are only a few  
 251 contacts between cement particles, this small contact surface corresponds to low storage moduli.  
 252 As the anhydrous cement particle are covered with hydrates, the contact surface increases and the  
 253 storage modulus increases too.



254

255 **Fig. 9. Evolution of the storage modulus  $G'$  with hydration time (cement paste with  $w/c=0.45$ )**

256 Furthermore, as shown in Fig. 10, calcite suspension exhibits a linear viscoelastic domain with a  
 257 critical strain of the order of few hundredths ( $10^{-2}$  %), as in fresh cement paste. This critical strain  
 258 cannot be explained by the formation of hydrates, since calcite suspension is chemically inert.  
 259 The interacting particles network in such suspension is principally due to the colloidal attractive  
 260 forces and to direct contacts between particles [29].



261

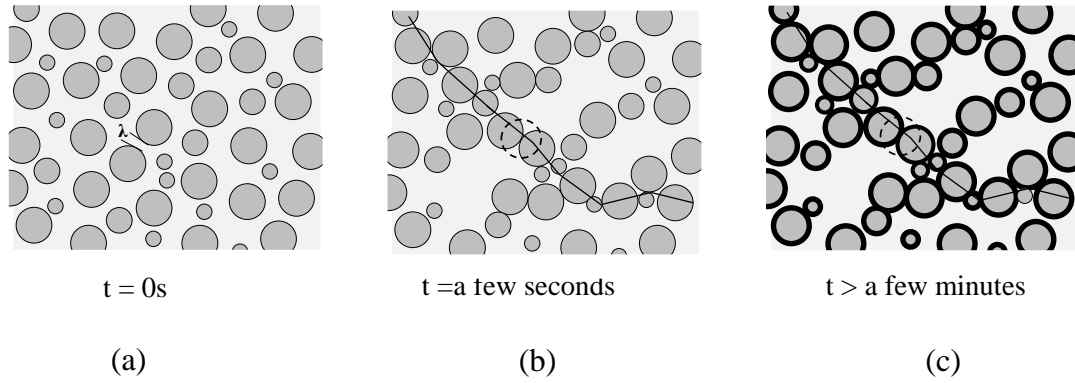
262 **Fig. 10. Storage and loss moduli in calcite suspension with water to solid ratio of 0.35**

263 According to these observations, the effect of  $w/c$  ratio and SP dosage on the deformation capacity  
 264 of fresh cement pastes could be explained. In fact, as shown in Fig. 11-a, immediately after the



265 end of mixing, the cement paste is a concentrated suspension of more or less dispersed particles.  
266 The average spacing between cement particles ( $\lambda$  in Fig. 11-a) is of the order of  $\mu\text{m}$  [34,35]. Guo  
267 et al [34] found, through yield stress calculations, that the distance between cement particles is  
268 ranging from 2.5 to 5  $\mu\text{m}$ , while Zhu et al. [35] obtained an average spacing between cement  
269 particles ranging from 0.9 to 1.4  $\mu\text{m}$ . It is worth noting that this distance depends strongly on w/c  
270 ratio and particle size distribution.

271 After a few seconds, which corresponds to the characteristic time of flocculation [8], a  
272 flocculation occurs due to colloidal attractive forces which lead to the formation of a network of  
273 interacting particles that occupies the entire volume of the sample; i.e. there exist a continuous  
274 percolation path able to withstand a minimum stress (Fig. 11-b). The behavior of cement paste  
275 kept at rest tends towards a solid-like behavior. As the hydration progresses (after few minutes),  
276 the early hydrates (in red in Fig. 11), which preferentially form on the surface of the anhydrous  
277 phases, increase the contact between cement particles (Fig. 11-c). Zingg et al. [26] found that in  
278 the absence of superplasticizer, early hydrates tend to precipitate immediately after mixing on  
279 clinker surfaces forming hydration rims leading to agglomeration and interlocking bridges.  
280 However, in the presence of superplasticizer, the early hydrates precipitate in the pore solution  
281 and the agglomeration is limited. In addition, the thickness of hydration rims around the clinker  
282 grains is more greater in the absence of superplasticizer [26]. The separation distance between  
283 cement particles ( $h$  in Fig. 12) after agglomeration is of the order of nm [13,15,31]. Values ranging  
284 from 5 to 10 nm can be found in the literature. This separation distance depends on the  
285 conformation of superplasticizer [36,37]. It has to be kept in mind that as the hydration progresses,  
286 the dissolution of anhydrous cement increases and leads to an increase in the number of fine  
287 particles and an increase in ionic strength which enhances flocculation [38,39].

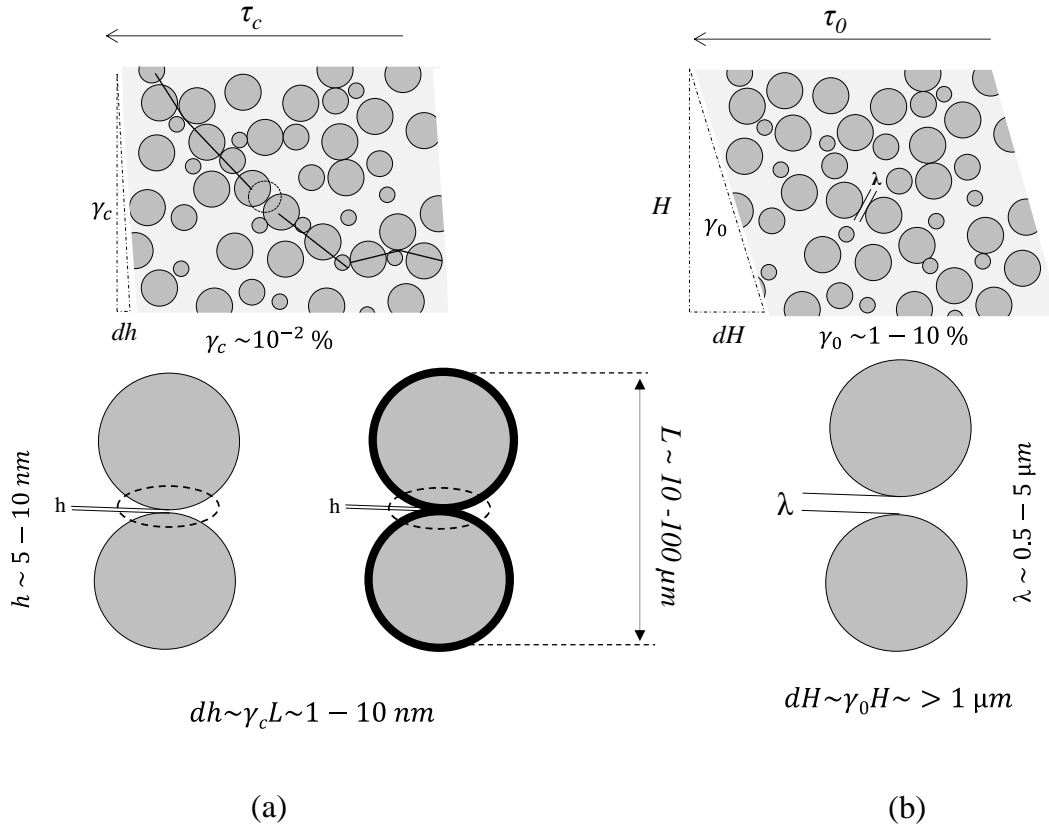


288

289 **Fig. 11. Illustration of the formation of a percolation path: (a) cement paste immediately after the**  
 290 **end of the mixing, (b) few seconds after the mixing, (c) few minutes after the mixing (in bold: early**  
 291 **hydrates)**

292 The application of shear stress, a few seconds or a few minutes after mixing, induces a  
 293 macroscopic deformation that can be described at the local scale by the relative movement of two  
 294 neighboring cement particles [8]. When the critical strain ( $\gamma_c$ ) is reached, the continuous  
 295 percolation path is broken locally (change in the particle/particle contact), but this does not mean  
 296 that the flow is initiated [15]. In fact, this critical strain of the order of  $10^{-2}$  % is consistent with a  
 297 change in the separation distance ( $h$ ) as illustrated in Fig. 12-a (of the order of nm) [8]. However,  
 298 the largest strain  $\gamma_0$  (peak in the shear stress-strain curve or transition strain in oscillatory  
 299 measurement) describes large structural changes and reorganizations of cement particles in the  
 300 shear plane corresponding to the initiation of flow. Thus, when the largest strain is reached,  
 301 cement paste behaves like a liquid (steady state flow) and tend towards the dispersion state  
 302 illustrated in Fig. 11-a. Thus, the largest strain involves a large change of the order of  $\mu\text{m}$  as  
 303 illustrated in Fig. 12-b.

304 It thus appears that the macroscopic shear strain is closely related to the interparticle distance  
 305 between cement particles which dictates the deformation capacity. This interparticle distance  
 306 depends on several factors such as solid volume fraction and superplasticizer dosage, and  
 307 conditions the magnitude of interparticle forces. However, when a percolation path is formed, the  
 308 interparticle distance ( $h$ ) depends only on the presence of superplasticizer [13,33].



309

310 **Fig. 12. Illustration of the formation of a percolation path and the shearing of a cement paste (in**  
 311 **bold: early hydrates)**

312 The critical strain  $\gamma_c$  is strongly affected by SP dosage. In fact, the electrosteric effect induced by  
 313 the presence of superplasticizer leads to increase of separation distance ( $h$ ) and thus to the  
 314 decrease of the magnitude of attractive forces [13,33]. This could explain the increase of the  
 315 deformation capacity of cement paste with superplasticizer, and thereby the variation of the  
 316 critical strain. However, this critical strain is slightly affected by w/c ratio (in the usual  
 317 concentration range). In fact, when flocculation occurs, the separation distance ( $h$ ) depends very  
 318 slightly on w/c ratio [33].

319 Furthermore, the largest strain ( $\gamma_0$ ) associated with the flow onset seems to be more influenced  
 320 by w/c ratio. It increases with decreasing w/c ratio [1] (Fig. 4). As reported by Guo et al. [34], the  
 321 average spacing between cement particles increases with w/c ratio. The effect of w/c ratio on the  
 322 largest strain (or transition strain) could be explained by the deformation capacity. In fact,  
 323 increasing the solid volume fraction leads to an increase of the number of particles which may be  
 324 approximately estimated as  $\phi d^{-3}$  ( $\phi$  is the solid volume fraction and  $d$  is the mean diameter) [8].

325 This results in the decrease of the average spacing between particles [34] and the strain required  
326 to initiate the flow and to induce large structural changes is expected to increase.

## 327 **4 Conclusions**

328 Rheological characterizations using oscillatory method and yield stress measurements were  
329 performed to examine the deformation capacity of fresh cement pastes. The effect of w/c ratio  
330 and admixture on these viscoelastic properties can help to better understand the origins of the  
331 deformation capacity of fresh cement paste.

332 It was shown that water to cement ratio has no effect on the critical strain at the end of the LVED,  
333 but decreases the storage modulus. This reflects the decrease of the cement paste stiffness.

334 Furthermore, SP dosage was found to have a strong effect on the LVED. In fact, the increase of  
335 SP dosage leads to the increase of the critical strain and the decrease of the storage modulus  
336 reflecting an enhanced dispersion of cement particles.

337 The critical strain at the end of the LVED and the smallest strain in the shear stress-strain curve  
338 obtained by yield stress measurement could be associated with strong physical forces (colloidal  
339 forces enhanced by early hydrates formation), while the transition strain ( $G' = G''$ ) and the largest  
340 strain in yield stress measurement could be associated with large structural reorganizations  
341 leading to the flow onset.

## 342 **Declarations**

### 343 **Funding**

344 No funds, grants, or other support was received.

### 345 **Conflicts of interests/Competing interests**

346 The author has no conflicts to disclose.

## 347 **References**

348 [1] D. Jiao, G. De Schutter, Insights into the viscoelastic properties of cement paste based on

- 349 SAOS technique, *Constr. Build. Mater.* 357 (2022) 129320.  
350 doi:<https://doi.org/10.1016/j.conbuildmat.2022.129320>.
- 351 [2] K. Zhang (K), A. Mezhov, W. Schmidt, Chemical and thixotropic contribution to the  
352 structural build-up of cementitious materials, *Constr. Build. Mater.* 345 (2022) 128307.  
353 doi:<https://doi.org/10.1016/j.conbuildmat.2022.128307>.
- 354 [3] A.M. Mostafa, A. Yahia, New approach to assess build-up of cement-based suspensions,  
355 *Cem. Concr. Res.* 85 (2016) 174–182.  
356 doi:<https://doi.org/10.1016/j.cemconres.2016.03.005>.
- 357 [4] M.A. Schultz, L.J. Struble, Use of oscillatory shear to study flow behavior of fresh  
358 cement paste, *Cem. Concr. Res.* 23 (1993) 273–282. doi:10.1016/0008-8846(93)90092-  
359 N.
- 360 [5] Q. Yuan, D. Zhou, K.H. Khayat, D. Feys, C. Shi, On the measurement of evolution of  
361 structural build-up of cement paste with time by static yield stress test vs. small  
362 amplitude oscillatory shear test, *Cem. Concr. Res.* 99 (2017) 183–189.  
363 doi:<https://doi.org/10.1016/j.cemconres.2017.05.014>.
- 364 [6] M. Thiedeitz, T. Kränkel, C. Gehlen, Viscoelastoplastic classification of cementitious  
365 suspensions: transient and non-linear flow analysis in rotational and oscillatory shear  
366 flows, *Rheol. Acta.* 61 (2022) 549–570. doi:10.1007/s00397-022-01358-9.
- 367 [7] F. Mahaut, S. Mokéddem, X. Chateau, N. Roussel, G. Ovarlez, Effect of coarse particle  
368 volume fraction on the yield stress and thixotropy of cementitious materials, *Cem.*  
369 *Concr. Res.* 38 (2008) 1276–1285. doi:10.1016/j.cemconres.2008.06.001.
- 370 [8] N. Roussel, G. Ovarlez, S. Garrault, C. Brumaud, The origins of thixotropy of fresh  
371 cement pastes, *Cem. Concr. Res.* 42 (2012) 148–157.  
372 doi:10.1016/j.cemconres.2011.09.004.
- 373 [9] Y. El Bitouri, N. Azéma, Potential Correlation Between Yield Stress and Bleeding, in:

- 374 SP-349 11th ACI/RILEM Int. Conf. Cem. Mater. Altern. Bind. Sustain. Concr.,  
375 American Concrete Institute, 2022: pp. 479–494. doi:10.14359/51732766.
- 376 [10] W.-G. Lei, L.J. Struble, Microstructure and Flow Behavior of Fresh Cement Paste, J.  
377 Am. Ceram. Soc. 80 (1997) 2021–2028. doi:https://doi.org/10.1111/j.1151-  
378 2916.1997.tb03086.x.
- 379 [11] L. Nachbaur, J.C. Mutin, A. Nonat, L. Choplin, Dynamic mode rheology of cement and  
380 tricalcium silicate pastes from mixing to setting, Cem. Concr. Res. 31 (2001) 183–192.  
381 doi:10.1016/S0008-8846(00)00464-6.
- 382 [12] J.T. Kolawole, R. Combrinck, W.P. Boshoff, Rheo-viscoelastic behaviour of fresh  
383 cement-based materials: Cement paste, mortar and concrete, Constr. Build. Mater. 248  
384 (2020) 118667. doi:https://doi.org/10.1016/j.conbuildmat.2020.118667.
- 385 [13] A. Perrot, T. Lecompte, H. Khelifi, C. Brumaud, J. Hot, N. Roussel, Yield stress and  
386 bleeding of fresh cement pastes, Cem. Concr. Res. 42 (2012) 937–944.  
387 doi:10.1016/j.cemconres.2012.03.015.
- 388 [14] N. Roussel, Steady and transient flow behaviour of fresh cement pastes, Cem. Concr.  
389 Res. 35 (2005) 1656–1664. doi:10.1016/j.cemconres.2004.08.001.
- 390 [15] N. Roussel, A. Lemaître, R.J. Flatt, P. Coussot, Steady state flow of cement suspensions:  
391 A micromechanical state of the art, Cem. Concr. Res. 40 (2010) 77–84.  
392 doi:10.1016/j.cemconres.2009.08.026.
- 393 [16] M. Fourmentin, G. Ovarlez, P. Faure, U. Peter, D. Lesueur, D. Daviller, P. Coussot,  
394 Rheology of lime paste—a comparison with cement paste, Rheol. Acta. 54 (2015) 647–  
395 656. doi:10.1007/s00397-015-0858-7.
- 396 [17] Y. El Bitouri, N. Azéma, On the ‘Thixotropic’ Behavior of Fresh Cement Pastes, Eng. 3  
397 (2022) 677–692. doi:10.3390/eng3040046.
- 398 [18] Z. Zhang, J. Xiao, K. Han, J. Wang, X. Hu, Study on the structural build-up of cement-

- 399 ground limestone pastes and its micro-mechanism, *Constr. Build. Mater.* 263 (2020)  
400 120656. doi:<https://doi.org/10.1016/j.conbuildmat.2020.120656>.
- 401 [19] A. Perrot, D. Rangeard, A. Pierre, Structural built-up of cement-based materials used for  
402 3D-printing extrusion techniques, *Mater. Struct. Constr.* 49 (2016) 1213–1220.  
403 doi:10.1617/s11527-015-0571-0.
- 404 [20] Q. Yuan, D. Zhou, B. Li, H. Huang, C. Shi, Effect of mineral admixtures on the  
405 structural build-up of cement paste, *Constr. Build. Mater.* 160 (2018) 117–126.  
406 doi:<https://doi.org/10.1016/j.conbuildmat.2017.11.050>.
- 407 [21] Z. Zhang (Z), Z. Jia, J. Shi, Y. Jiang, N. Banthia, Y. Zhang, Clarifying and quantifying  
408 the driving force for the evolution of static yield stress of cement pastes, *Cem. Concr.*  
409 *Res.* 167 (2023) 107129. doi:<https://doi.org/10.1016/j.cemconres.2023.107129>.
- 410 [22] A.M. Mostafa, A. Yahia, Physico-chemical kinetics of structural build-up of neat  
411 cement-based suspensions, *Cem. Concr. Res.* 97 (2017) 11–27.  
412 doi:10.1016/j.cemconres.2017.03.003.
- 413 [23] Y. El Bitouri, The Effect of Temperature on the Structural Build-Up of Cement Pastes,  
414 *CivilEng.* 4 (2023) 1198–1213. doi:10.3390/civileng4040066.
- 415 [24] K. Sujata, H.M. Jennings, Formation of a Protective Layer During the Hydration of  
416 Cement, *J. Am. Ceram. Soc.* 75 (1992) 1669 – 1673. doi:10.1111/j.1151-  
417 2916.1992.tb04243.x.
- 418 [25] S. Gauffinet, É. Finot, E. Lesniewska, A. Nonat, Direct observation of the growth of  
419 calcium silicate hydrate on alite and silica surfaces by atomic force microscopy;  
420 [Observation directe de la croissance d’hydrosilicate de calcium sur des surfaces d’alite  
421 et de silice par microscopie a force atomique], *Comptes Rendus l’Academie Sci. - Ser.*  
422 *Ila Sci. La Terre Des Planetes.* 327 (1998) 231 – 236. doi:10.1016/S1251-  
423 8050(98)80057-8.

- 424 [26] A. Zingg, L. Holzer, A. Kaech, F. Winnefeld, J. Pakusch, S. Becker, L. Gauckler, The  
425 microstructure of dispersed and non-dispersed fresh cement pastes — New insight by  
426 cryo-microscopy, *Cem. Concr. Res.* 38 (2008) 522–529.  
427 doi:<https://doi.org/10.1016/j.cemconres.2007.11.007>.
- 428 [27] N. Mikanovic, C. Jolicoeur, Influence of superplasticizers on the rheology and stability  
429 of limestone and cement pastes, *Cem. Concr. Res.* 38 (2008) 907–919.  
430 doi:[10.1016/j.cemconres.2008.01.015](https://doi.org/10.1016/j.cemconres.2008.01.015).
- 431 [28] A. Tramaux, N. Azéma, Y. El Bitouri, G. David, C. Negrell, A. Poulesquen, J. Haas, S.  
432 Remond, Synthesis of phosphonated comb-like copolymers and evaluation of their  
433 dispersion efficiency on CaCO<sub>3</sub> suspensions part II: Effect of macromolecular structure  
434 and ionic strength, *Powder Technol.* 334 (2018) 163–172.  
435 doi:[10.1016/j.powtec.2018.04.020](https://doi.org/10.1016/j.powtec.2018.04.020).
- 436 [29] T. Liberto, M. Le Merrer, C. Barentin, M. Bellotto, J. Colombani, Elasticity and yielding  
437 of calcite paste: scaling laws in a dense colloidal suspension, *Soft Matter.* 13 (2017).  
438 doi:[10.1039/C6SM02607A](https://doi.org/10.1039/C6SM02607A).
- 439 [30] F. Mahaut, X. Chateau, P. Coussot, G. Ovarlez, Yield stress and elastic modulus of  
440 suspensions of noncolloidal particles in yield stress fluids, *J. Rheol. (N. Y. N. Y.)* 52  
441 (2008) 287–313. doi:[10.1122/1.2798234](https://doi.org/10.1122/1.2798234).
- 442 [31] R.J. Flatt, P. Bowen, Yodel: A yield stress model for suspensions, *J. Am. Ceram. Soc.* 89  
443 (2006) 1244–1256. doi:[10.1111/j.1551-2916.2005.00888.x](https://doi.org/10.1111/j.1551-2916.2005.00888.x).
- 444 [32] N. Roussel, H. Bessaies-Bey, S. Kawashima, D. Marchon, K. Vasilic, R. Wolfs, Recent  
445 advances on yield stress and elasticity of fresh cement-based materials, *Cem. Concr.*  
446 *Res.* 124 (2019) 105798. doi:[10.1016/j.cemconres.2019.105798](https://doi.org/10.1016/j.cemconres.2019.105798).
- 447 [33] R.J. Flatt, Dispersion forces in cement suspensions, *Cem. Concr. Res.* 34 (2004) 399–  
448 408. doi:[10.1016/j.cemconres.2003.08.019](https://doi.org/10.1016/j.cemconres.2003.08.019).



- 449 [34] Y. Guo, T. Zhang, J. Wei, Q. Yu, S. Ouyang, Evaluating the distance between particles  
450 in fresh cement paste based on the yield stress and particle size, *Constr. Build. Mater.*  
451 142 (2017) 109–116. doi:<https://doi.org/10.1016/j.conbuildmat.2017.03.055>.
- 452 [35] W. Zhu, Q. Feng, Q. Luo, J. Yan, C. Lu, Investigating the effect of polycarboxylate-  
453 ether based superplasticizer on the microstructure of cement paste during the setting  
454 process, *Case Stud. Constr. Mater.* 16 (2022) e00999.  
455 doi:<https://doi.org/10.1016/j.cscm.2022.e00999>.
- 456 [36] R.J. Flatt, I. Schober, E. Raphael, C. Plassard, E. Lesniewska, Conformation of adsorbed  
457 comb copolymer dispersants, *Langmuir.* 25 (2009) 845–855. doi:10.1021/la801410e.
- 458 [37] R.J. Flatt, Y.F. Houst, A simplified view on chemical effects perturbing the action of  
459 superplasticizers, *Cem. Concr. Res.* 31 (2001) 1169–1176. doi:10.1016/S0008-  
460 8846(01)00534-8.
- 461 [38] A. Bogner, J. Link, M. Baum, M. Mahlbacher, T. Gil-Diaz, J. Lützenkirchen, T.  
462 Sowoidnich, F. Heberling, T. Schäfer, H.-M. Ludwig, F. Dehn, H.S. Müller, M. Haist,  
463 Early hydration and microstructure formation of Portland cement paste studied by  
464 oscillation rheology, isothermal calorimetry, <sup>1</sup>H NMR relaxometry, conductance and  
465 SAXS, *Cem. Concr. Res.* 130 (2020) 105977.  
466 doi:<https://doi.org/10.1016/j.cemconres.2020.105977>.
- 467 [39] T.C. Powers, *The properties of fresh concrete*, J. Wiley Sons (Hoboken, NJ, USA).  
468 (1968) 533–652.
- 469